DEVELOPMENTAL DYNAMICS 245:1159–1175, 2016
DOI: 10.1002/DVDY.24457

RESEARCH ARTICLE

Head Regeneration in Hemichordates is not a Strict Recapitulation of Development

Shawn M. Luttrell,[1,2] Kirsten Gotting,[3] Eric Ross,[3,4] Alejandro Sánchez Alvarado,[3,4] and Billie J. Swalla[1,2]*

[1]Biology Department, University of Washington, Seattle, Washington
[2]Friday Harbor Laboratories, University of Washington, Friday Harbor, Washington
[3]Stowers Institute for Medical Research, Kansas City, Missouri
[4]Howard Hughes Medical Institute, Stowers Institute for Medical Research, Kansas City, Missouri

Background: Head or anterior body part regeneration is commonly associated with protostome, but not deuterostome invertebrates. However, it has been shown that the solitary hemichordate *Ptychodera flava* possesses the remarkable capacity to regenerate their entire nervous system, including their dorsal neural tube and their anterior head-like structure, or proboscis. Hemichordates, also known as acorn worms, are marine invertebrate deuterostomes that have retained chordate traits that were likely present in the deuterostome ancestor, placing these animals in a vital position to study regeneration and chordate evolution. All acorn worms have a tripartite body plan, with an anterior proboscis, middle collar region, and a posterior trunk. The collar houses a hollow, dorsal neural tube in ptychoderid hemichordates and numerous chordate genes involved in brain and spinal cord development are expressed in a similar anterior–posterior spatial arrangement along the body axis. **Results:** We have examined anterior regeneration in the hemichordate *Ptychodera flava* and report the spatial and temporal morphological changes that occur. Additionally, we have sequenced, assembled, and analyzed the transcriptome for eight stages of regenerating *P. flava*, revealing significant differential gene expression between regenerating and control animals. **Conclusions:** Importantly, we have uncovered developmental steps that are regeneration-specific and do not strictly follow the embryonic program. *Developmental Dynamics 245:1159–1175, 2016.* © 2016 The Authors. Developmental Dynamics published by Wiley Periodicals, Inc. on behalf of American Association of Anatomists

Key words: hemichordate; *Ptychodera flava*; regeneration; transcriptome; deuterostome

Submitted 15 January 2016; First Decision 4 September 2016; Accepted 5 September 2016; Published online 20 September 2016

Introduction

Regeneration has captured the interest and imagination of people for centuries. Popularized in myths, science fiction, and even horror movies, regeneration of missing and damaged tissue is a common reality in the animal kingdom. Nearly every animal phyla contains at least some species that consistently regenerate all or certain tissues and structures (Bely and Nyberg, 2010; Somorjai et al., 2012; Giangrande and Licciano, 2014). All deuterostome groups, with the possible exception of Xenoturbella, have at least some species with the capacity to regenerate (Sánchez Alvarado, 2000). Numerous chordates, including lancelets, tunicates, frogs, fish, salamanders, and even humans are able to regenerate to some degree (Brown et al., 2009; Bely and Nyberg, 2010; Somorjai et al., 2012; Giangrande and Licciano, 2014). Every extant class of echinoderms have been reported to regenerate (Candia Carnevali et al., 2009), while some species of hemichordates, which are a sister group to the echinoderms, undergo asexual reproduction and regenerate all anterior and posterior body parts when amputated (Willey 1899; Dawydoff 1902; Rao 1954; Rychel and Swalla, 2008; Humphreys et al., 2010; Miyamoto and Saito, 2010).

When and in what animal lineage did the ability to regenerate first evolve? Was regeneration a stem metazoan trait that was subsequently lost or reduced in numerous taxa or has regeneration evolved independently several times across the metazoans? Porifera (Bely and Nyberg, 2010; Giangrande and Licciano, 2014), Cnidaria (Bosch, 2007; Dubuc et al., 2014), Ctenophora (Ryan et al., 2013; Moroz et al., 2014), and Placozoa (Bely and Nyberg, 2010) have extensive regenerative abilities and, as basal metazoans, these lineages suggest an ancient and ancestral mechanism of regeneration. Comparing gene regulatory networks used during regeneration across various animal phyla will help to elucidate common molecular mechanisms of regeneration.

Understanding the morphological and genetic basis of regeneration may yield clues to unlocking regeneration in animals with limited or no regenerative abilities, like humans. Millions of

Grant sponsor: DGE; Grant number: 1256082; Grant sponsor: NIH; Grant number: R37GM057260; Grant sponsor: HHMI; Grant sponsor: DBI; Grant number: 0939454; Grant sponsor: Seeley Fund for Ocean Research on Tetiaroa.
*Correspondence to: Billie J. Swalla, Biology Department, University of Washington, Seattle, WA 98195-1800. E-mail: bjswalla@u.washington.edu

Article is online at: http://onlinelibrary.wiley.com/doi/10.1002/dvdy.24457/abstract

people suffer from neurodegenerative diseases, spinal cord injuries, and limb amputations (Brown et al., 2005; Ziegler-Graham et al., 2008; Mahabaleshwarkar and Khanna, 2014). Furthermore, aging and age-related diseases will eventually affect everyone. Regeneration may slow the aging process and stem cells present one feasible way to combat a multitude of diseases and injuries (Rando and Wyss-Coray, 2014). If regeneration is a stem deuterostome trait, it is likely that humans possess many, if not all, of the genetic switches controlling regeneration, but those switches have been modified or inactivated in some way over evolutionary time. It may, therefore, be possible to re-activate those pathways in humans using information gained from studying genetic models made from animals with extensive regenerative capabilities.

We are seeking to identify the morphological and genetic underpinnings controlling regeneration in the solitary hemichordate, *Ptychodera flava* (Eschscholtz, 1825), which is a basal deuterostome and capable of regenerating all anterior and posterior structures when bisected (Rychel and Swalla, 2008; Humphreys et al., 2010). It is critical to know when internal structures regenerate to use genetic knock downs and knock outs, as well as overexpression, to characterize the function of genes directing the regeneration process. Moreover, hemichordates are the only deuterostome known to be able to regenerate an anterior head-like structure and entire central nervous system (CNS). *Ptychodera flava* progresses from a fertilized embryo to a planktonic, feeding larva that can remain in the water column for up to 300 days (Hadfield, 1978; Lin et al., 2016). Upon metamorphosis, the larva develops into a juvenile worm that settles to the ocean floor to begin a benthic lifestyle. Solitary hemichordates are exclusively marine and adult animals have a tripartite body plan with an anterior proboscis that is used for digging and burrowing in the sand and mud, a middle collar region with a hollow, dorsal neural tube in ptychoderid hemichordates, a ventral mouth between the proboscis and collar, and a long posterior trunk with pharyngeal gill slits and gonads in the anterior trunk, a hepatic region in the mid-trunk and a terminal anus (Balser and Ruppert, 1990; Brown et el., 2008; Luttrell and Swalla, 2014).

The hemichordate nervous system is quite interesting. Upon embryogenesis in direct developing hemichordates and metamorphosis in indirect developers, dorsal and ventral nerve cords develop along the full length of the trunk and nerve rings form around the base of the collar and the base of the proboscis (Balser and Ruppert, 1990; Kaul and Stach, 2010; Miyamoto et al., 2010; Miyamoto and Wada, 2013; Kaul-Strehlow et al., 2015). Adult echinoderms also develop nerve cords throughout each arm and a circumferential nerve ring around the central disc; however, it still remains to be determined whether echinoderm and hemichordate nerve cords are homologous structures (Sly et al., 2002; Holland et al., 2013). In addition to nerve cords, *P. flava* also develops a hollow, neural tube that is positioned dorsally in the collar region. Our lab has shown this structure forms from ectoderm that invaginates and rolls up forming a hollow tube, similar to chordate neurulation (Morgan, 1894; Luttrell et al., 2012; Miyamoto and Wada, 2013; Luttrell and Swalla, 2014).

Lastly, hemichordates have a diffuse nerve net throughout the ectoderm, similar to the adult tunicate, *Ciona intestinalis* (Balser and Ruppert, 1990; Lowe et al., 2003; Dahlberg et al., 2009; Miyamoto et al., 2010; Kaul-Strehlow et al., 2015). The adult acorn worm, in light of these similarities, has aspects of the different types of nervous systems that are present in the deuterostomes. Remarkably, *P. flava* is able to regenerate all of these structures, making hemichordates a model system to study nervous system evolution and regeneration in this clade of animals. Furthermore, as invertebrates, hemichordates lack the numerous genome duplications events present in the vertebrates (Dehal and Boore, 2005; Hughes and Liberles, 2008), thereby making functional studies of the regeneration genes more tractable in this animal.

Here, we report the spatial and temporal regeneration of internal body structures to complement the previously published external morphology regeneration data (Willey, 1899; Rao, 1954; Nishikawa, 1977; Rychel and Swalla, 2008; Humphreys et al., 2010). We also include analyses of the transcriptome from regenerating *P. flava* animals. In total, eight different stages of regeneration were sequenced, assembled, and annotated to track changes in early gene expression that direct regeneration of anterior structures. We document expression profiles and gene ontologies of hundreds of putative genes associated with anterior head regeneration. These data build a foundation for future experiments that may show what genes are sufficient and necessary to start the regeneration program in *P. flava*. Our morphological data shows the regenerative response to these early changes in gene expression and we document complete anterior regeneration of the proboscis, collar, and anterior trunk. Furthermore, we uncovered morphological differences between early development and regeneration of anterior structures, including the neural tube. The assembled transcriptomes reported here not only complement recent *P. flava* developmental transcriptomes (Shu-Hwa et al., 2014; Tagawa et al., 2014; Simakov et al., 2015), but also open the door to systematic comparisons of embryonic processes to regenerative events in hemichordates specifically, and deuterostomes in general.

Results

Regeneration of External and Internal Anterior Features in *P. flava*

Intact, healthy, adult worms (Fig. 1A) were bisected in the trunk between the branchial region and the hepatic sacs (Fig. 1B) and the posterior piece was monitored for regeneration signs at the cut site (Fig. 1C). The first observable change in tissue composition in *Ptychodera flava* is wound healing. This process is relatively rapid and takes place within the first 2 days following amputation at 26°C. Wound healing culminates in ectoderm covering and sealing the open cut site (Fig. 1D–F). Over the next 3 days, a regeneration blastema forms at the anterior end (Fig. 1G,H). Cells accumulate and proliferate in the blastema to yield a new, rudimentary anterior head, or proboscis (Fig. 1I). Between days 4 and 5 post bisection, the mouth has opened on the ventral side (Figs. 1J, 3D1–3).

Over the next several days, cells continue to proliferate enlarging the proboscis and the collar begins to wrap around the base of the proboscis (Fig. 1K–T). The collar regenerates in the ventral and lateral positions first (Fig. 1K–P). Gill slits and gill bars start to form in the anterior most region of the trunk after 10 to 12 days, before the collar ectoderm completely regenerates and closes on the dorsal side (Fig. 1Q–T). At 13 days post bisection, the ventral and lateral collar ectoderm has fully regenerated (Fig. 2). The dorsal most region of the collar has not yet formed, but will continue to regenerate and finally close forming a continuous ring around the neck region after approximately 2 weeks of regeneration. The epibranchial nerve ring that that wraps around the posterior collar is visible in the newly regenerated tissue and

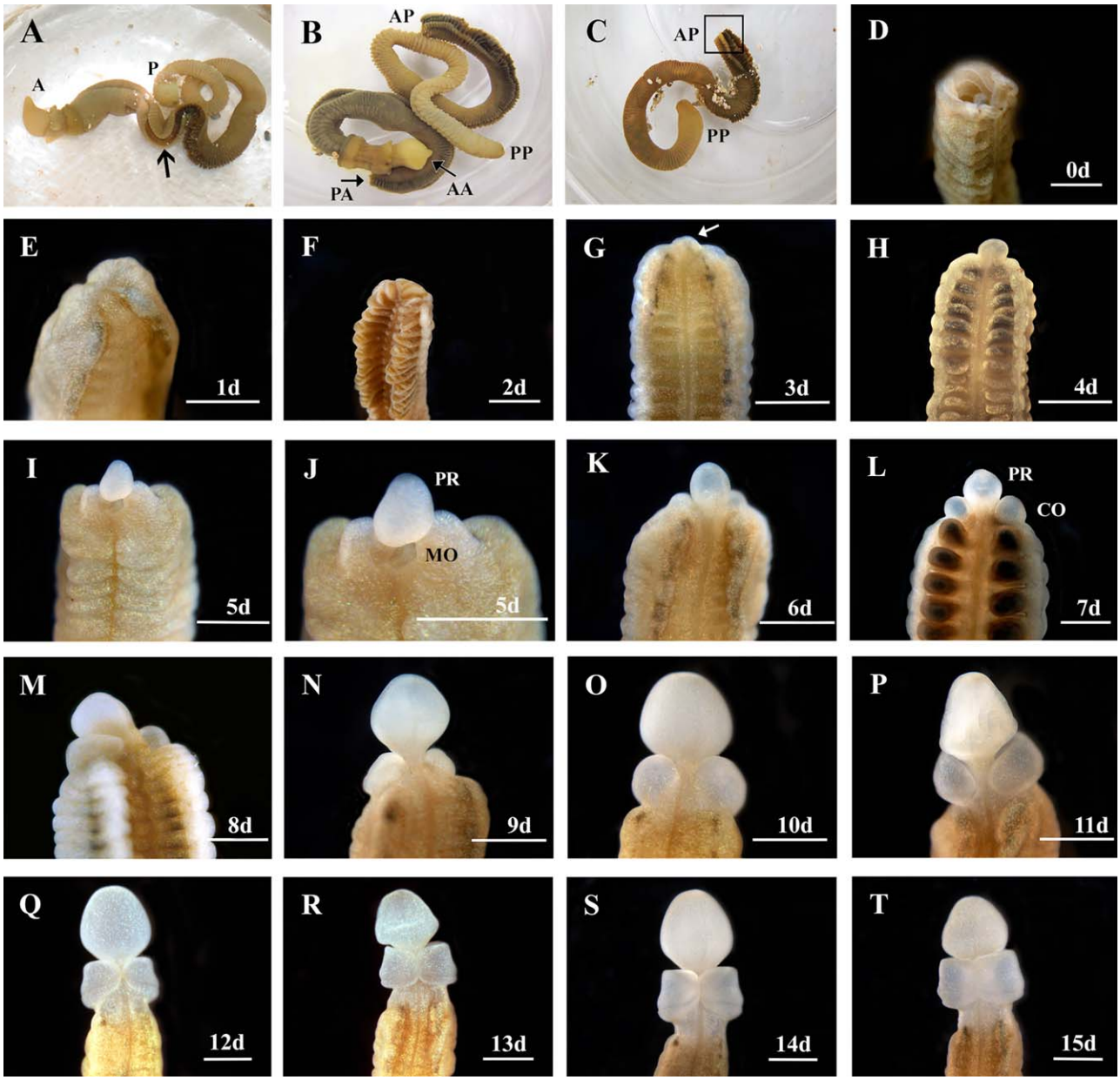

Fig. 1. Regenerating anterior structures on *Ptychodera flava*. **A:** An intact, live animal. Anterior is to the left. The arrow indicates where the animal will be bisected. a = anterior, p = posterior. **B:** A bisected animal. AA, anterior end of the anterior half; PA, posterior end of the anterior half; AP, anterior end of the posterior half; PP, posterior end of the posterior half. **C:** The posterior half of the animal. The boxed area is the site of regeneration. **D:** The cut site of the posterior half of the animal. **E–H:** One day (1d) through 4 days (4d) postcut, showing the open wound has healed and a regeneration blastema has formed in two different animals. The arrow in (G) marks the blastema. **I,J:** At 5 days post bisection (5d), the blastema has formed a rudimentary proboscis (PR) and the mouth (MO) is open on the ventral side. **K–T:** Six days (6d) through 15 days (15d) show the proboscis (PR) the collar (CO) regenerating around the proboscis stalk in a ventral to dorsal manner. All views are dorsal and anterior is to the top except I, J, which are ventral views. Scale bars = 1 mm.

forms as the collar regrows and not after the collar has fully shaped (Fig. 2).

The internal regeneration morphology of *P. flava* is striking after the first day the animal is bisected. Both ectoderm and endoderm of the trunk region come together at the cut site and form a near continuous layer (Fig. 3A1). The folds of pre-existing endoderm are still present and the neural net is maintained below the ectoderm (Fig. 3A1). Existing muscle fibers of the trunk are still obvious at the anterior end where the wound has sealed (Fig. 3A1). Hepatic collagen is visible below the ectoderm at the cut site, denoting endoderm of the existing hepatic sacculations are taking part in wound healing (Fig. 3A1). On day 2 of regeneration, the wound has completely healed and the ectoderm epithelium is smooth and continuous (Fig. 3B1,B2). Dorsal and ventral blood vessels run the length of the animal, allowing blood cells to circulate. Blood is visible in the dorsal and ventral endoderm of the cut site, indicating that both blood vessels are likely supplying blood to this region (Fig. 3B2).

Hepatic collagen is still visible in the dorsal endoderm, suggesting that at least parts of this tissue have not undergone apoptosis

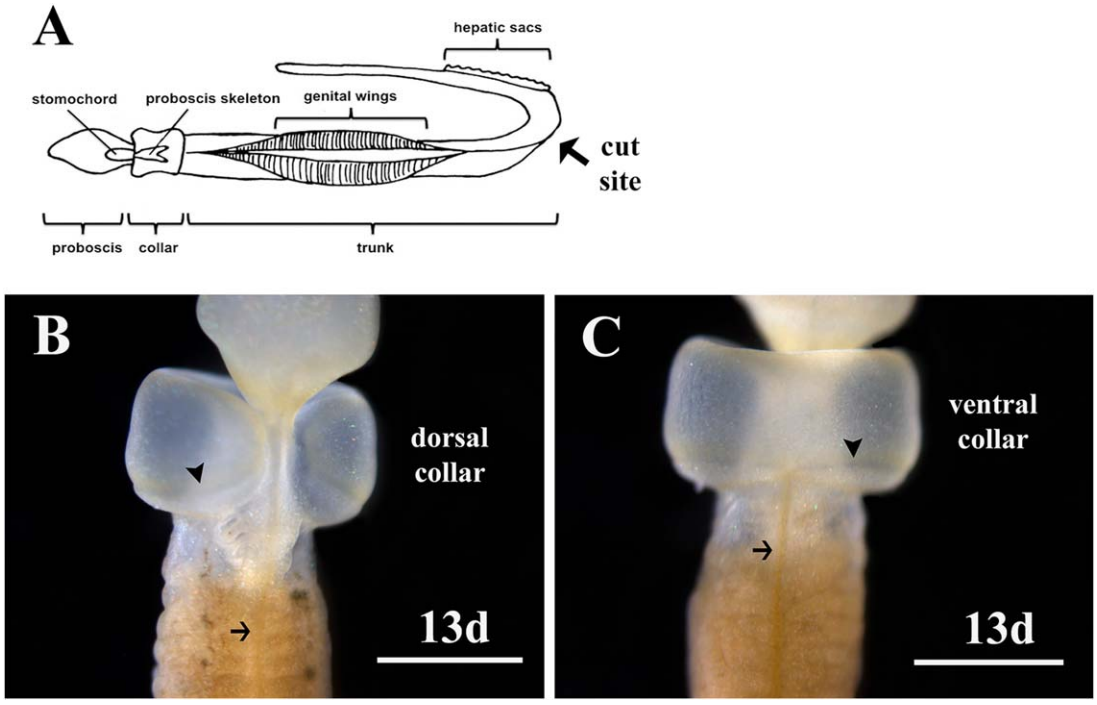

Fig. 2. Regenerating collar on *Ptychodera flava* at 13 days (13d) postamputation. **A:** An illustration showing the cut site in the trunk between the genital wings and the hepatic sacs. **B:** Dorsal view showing the collar has not completely closed and regeneration is incomplete. Three gill slits have formed in the anterior trunk. **C:** Ventral view of the collar on the same animal showing complete closure and regeneration of the ectoderm. Arrows indicate the dorsal nerve cord in the trunk in (B) and the ventral nerve cord in (C). The arrowheads indicate the epibranchial nerve ring formed at the base of the collar. Scale bars are 1mm.

or have been remodeled at this stage. By day 3 of regeneration, the blastema has formed a rudimentary proboscis (Fig. 3C1–4). A nerve net is present below the ectoderm in this region, at least partially originating from the existing trunk tissue and not wholly regenerated de novo (Fig. 3C1–4). At this stage, a structure resembling the presumptive stomochord appears posterior to the rudimentary proboscis and also appears to be derived from endodermal tissue (Fig. 3C3,C4). The hepatic sacculations are clearly visible in the existing trunk denoting the dorsal side and a thick nerve net is still present on the ventral side below the ectoderm posterior to the cut site (Fig. 3C1–C4).

As the proboscis grows, anterior internal tissues continue to be elaborated. Hemichordates are tricoelomates, having separate coeloms in the proboscis, collar, and trunk regions. The proboscis coelom is fully formed after 4 days of regeneration (Fig. 3D1–3). The dorsal blood vessel flows anteriorly from the trunk, through the collar, ultimately forming the heart in the posterior proboscis (Benito and Pardos, 1997). The dorsal vessel has regenerated into the proboscis, filling the coelom with blood at 4 days postamputation (Fig. 3D1–3). The mouth, which was visible in the external morphology at day 5, is clearly open in sagittal sections at day 4 (Fig. 3D1–3). The stomochord is a stiff, rod-like structure in the posterior proboscis and provides structural support for the superimposing heart/kidney complex (Balser and Ruppert, 1990; Rychel and Swalla, 2008; Miyamoto and Wada, 2013). The stomochord is apparent in sections after 5 days of regeneration (Fig. 3E2–4). At this stage, the stomochord forms between the boundary where ectoderm and endoderm meet. At this time, the heart-kidney complex regenerates in the lateral and dorsal positions around the stomochord (Fig. 3E1–4). The dorsal blood vessel is obvious at this stage, flowing into the proboscis just above the stomochord where the heart/kidney complex is regenerating (Fig. 3E1–4). The ventral blood vessel is supplying blood and cells to the presumptive ventral collar coelom as well (Fig. 3E1–4). One day later, the regenerated collar coeloms can be seen in the dorsal and ventral regions (Fig. 3F1–4). The proboscis skeleton provides structure and support for the collar and overlying dorsal blood vessel and neural tube (Luttrell et al., 2012). The proboscis skeleton regenerates from endoderm in the collar region and is visible in endodermal inpocketing at 13 days postamputation (Fig. 4P). The hollow, dorsal neural tube, which is found only in the collar region in ptychoderid hemichordates, begins to form in the posterior collar as the ectoderm closes on the dorsal side at 13 days postbisection (Fig. 4T). These morphological regenerative events are summarized in Table 1.

Dynamic and Discrete Cohorts of Gene Expression Patterns Are Observed During Early Stages of Head Regeneration

Regeneration of these morphological structures is driven by a significant change in gene expression as evidenced by the transcriptome data. A line graph was constructed to show clusters of up-regulated, putative genes showing similar expression profiles along all time points sampled (Fig. 5A). Nearly all genes in cluster A are significantly up-regulated 2 hr after the animal is bisected; however, the expression level of these genes steadily and drastically declines beginning 6 hr into the regeneration process. A heatmap of cluster A identifies the individual, putative genes and their expression profile across all time points (Fig. 5B). Heatmaps of the genes in cluster B shows overall expression is near baseline

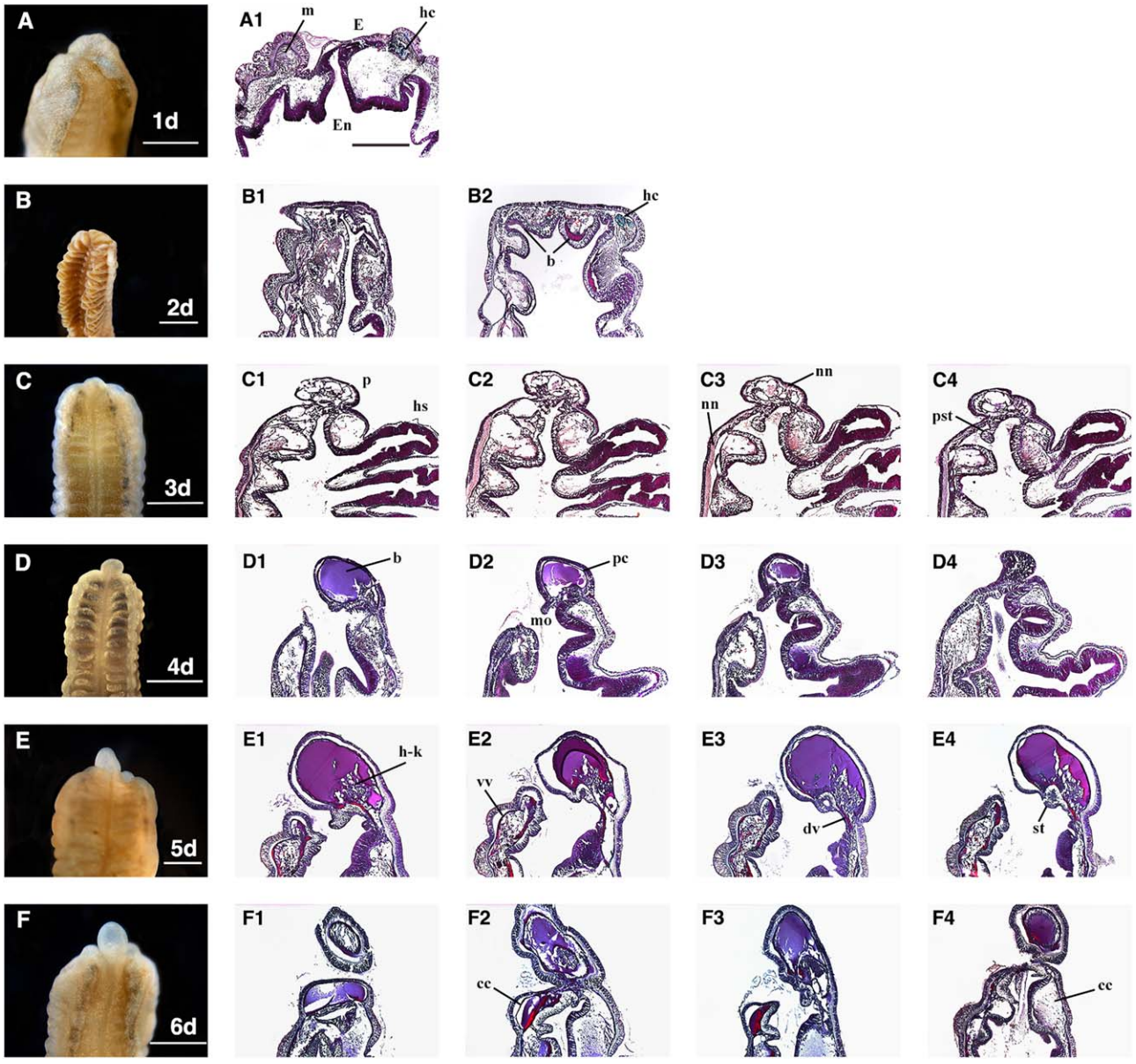

Fig. 3. A1–F4: Sagittal sections of *Ptychodera flava* anterior regeneration days 1–6 (A-F). Sections were made through the mid-sagittal area showing the internal morphology of proboscis and early collar regeneration. cc, collar coelom; dv, dorsal vessel; E, ectoderm; En, endoderm; hc, hepatic collagen; hs, hepatic sacculations; m, muscle; mo, mouth; nn, nerve net; p, proboscis; pc, proboscis coelom; pst, presumptive stomochord; st, stomochord; vv, ventral vessel. Scale bars = 1 mm and all sections are at the same magnification. All sections are anterior up and dorsal to the right and ventral to the left. All sections are stained with Milligan's trichrome stain. Collagen = green; nuclei, muscle = magenta.

values at the 2-hr time point, but then expression increases significantly after 6 hr and is elevated approximately 8-fold higher than control animals after 4 days of regeneration (Fig. 5C). Heatmaps of the cluster C and cluster D genes show similar expression profiles, both being only slightly elevated after 2 hr of regeneration and then progressively increasing until the 24-hr time point, at which time both clusters begin to show decreased expression levels, with cluster C displaying the most dramatic decrease (Fig. 5D,E). However, expression of putative genes in both clusters still remain over two log fold change higher than controls after 4 days of regeneration.

Down-regulated, putative genes were also identified and grouped into clusters of similar expression domains. A line graph shows four clusters of predicted genes with very different expression profiles (Fig. 6A). Heatmaps of cluster A show overall expression levels slightly below baseline values between 2 and 6 hr of regeneration and then expression gradually decreases with a steep decline between 3 and 4 days of regeneration. A detailed listing of these putative genes is included in Figure 7. Cluster B genes also start off at near baseline values and expression steadily decreases; however, this group of genes reverses at the 48-hr time point and expression levels begin to increase, although overall expression of this cluster remains significantly down-regulated at the 96-hr time point compared with control animals (Fig. 8).

Predicted genes in cluster C show an interesting expression pattern along all sampled time points. Expression is initially

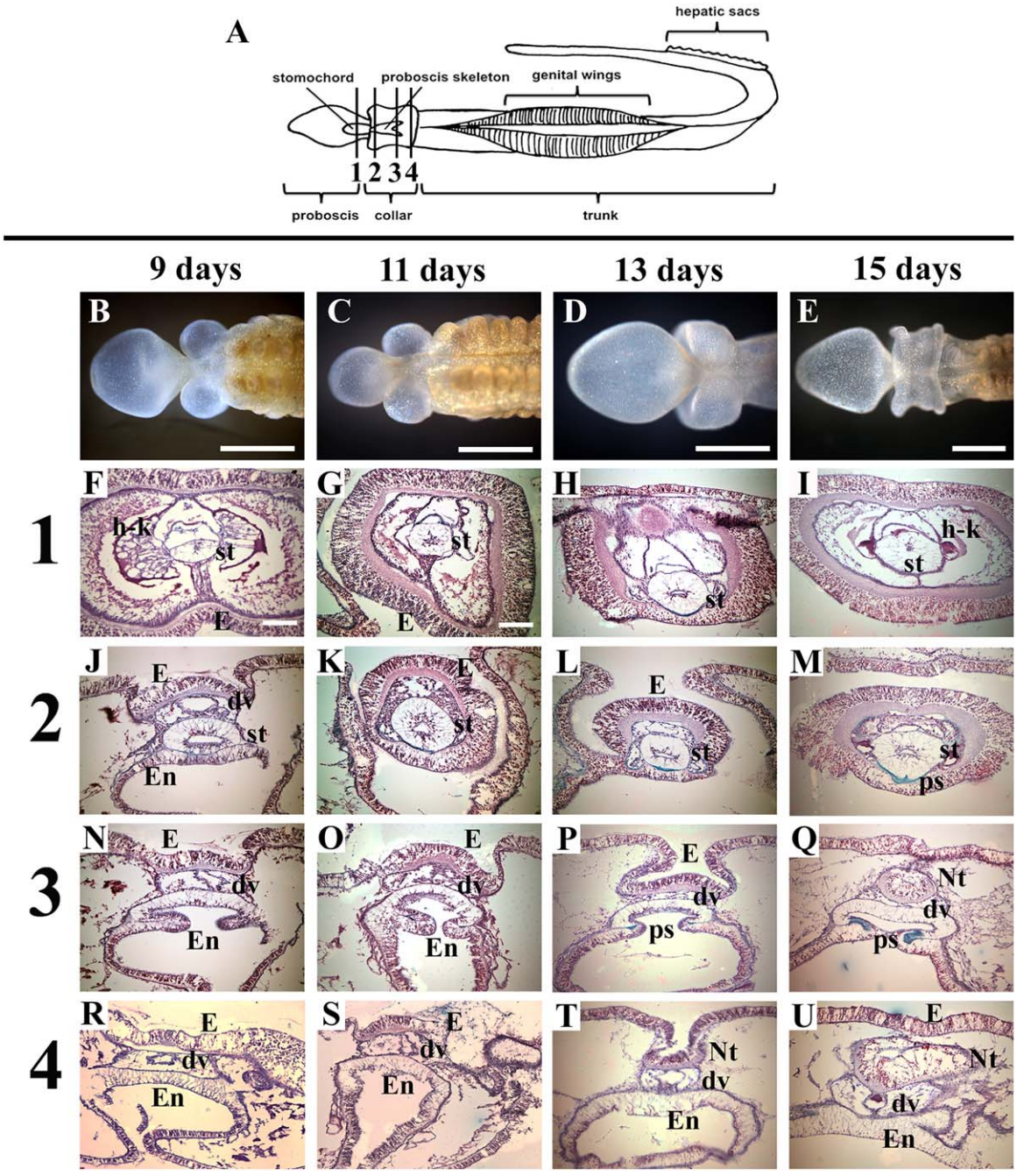

Fig. 4. Cross-sections of *Ptychodera flava* anterior regeneration days 9–15. All sections are stained with Milligan's trichrome at four different stages of regeneration: 9 days, 11 days, 13 days, and 15 days postamputation. **A:** Diagram of *P. flava* showing approximate locations of sections. Row (1) is taken through the posterior proboscis in all four regeneration stages. Row (2) is taken through the anterior collar. Row (3) is taken through the mid collar. Row (4) is taken through the posterior collar. dv, dorsal vessel; E, ectoderm; En, endoderm; h-k, heart-kidney complex; Nt, neural tube; ps, proboscis skeleton; st, stomochord. Scale bars = 1 mm in B–E; 0.1 mm in F–U. **B–U:** Dorsal views with anterior to the right in (B–E) and dorsal to the top in (F–U). All sections are stained with Milligan's trichrome stain. Collagen, green; nuclei, muscle = magenta.

significantly reduced by over three log fold compared with control animals at the 2-hr time point and then expression sharply increases over the next 2 hr, only to abruptly decrease again to nearly an 8-fold change from control animals at the 6-hr time point. Expression levels then steadily elevate again over the next 18 hr, at which point expression sharply declines again between 24 and 48 hr of regeneration, with expression values greater than 8-fold lower than control animals. Expression then rebounds over the next 48 hr and returns to around the same levels measured at the 2-hr time point, which is still nearly four log fold lower than expression in control animals (Fig. 6B). Cluster D genes are initially down-regulated after 2 hr of regeneration, but are significantly up-regulated from baseline levels at the 96-hr time point (Fig. 6C). Additionally, a heatmap was constructed for putative transcription factors and their relative expression compared with control animals over all time points (Fig. 9).

TABLE 1. Regeneration Timetable in *Ptychodera flava* at 26°C

Ptychodera flava anterior regeneration timetable at 26°C

	Days of regeneration						
Regeneration events	1-2	3-4	5-6	7-8	9-10	11-12	13-15
Wound healing	X						
PCNA positive cells (Rychel & Swalla, 2008)	X	X	X	X			
Nerve net	X	X					
Blastema		X					
Proboscis		X	X	X			
Proboscis coelom		X					
Dorsal vessel		X					
Mouth		X	X				
Stomochord			X	X			
Collar coelom			X				
Ventral and lateral collar			X	X	X	X	
Heart/kidney complex			X	X	X		
Proboscis skeleton						X	X
Gill slits						X	X
Dorsal collar							X
Neural tube							X

PCNA, proliferating cell nuclear antigen.

Gene Activity Associated With Cell Proliferation and Metabolic Changes is Prominently Detected in the Early Stages of *P. flava* Head Regeneration

Gene ontology (GO) analysis was completed to categorize the function of differentially expressed putative genes. We display the number of genes per significantly enriched GO term for 72 hr and 96 hr and no other time points because there was no enrichment for the other time points. Over half of the significantly enriched genes for which we have GO annotations play a role in cell proliferation and differentiation, as well as organ morphogenesis (Fig. 10A). Approximately 12% of the significantly enriched genes for which we have GO annotations are involved with cell signaling (Fig. 10A). Predicted orthologs of highly conserved developmental pathways were detected, including members of the Wnt signaling pathway, the fibroblast growth factor signaling pathway, and the Notch signaling pathway (Fig. 10A).

We further classified the amount of both up- and down-regulated genes at the 72-hr time point and 96-hr time point into biological processes, molecular function, and cellular component categories (Fig. 10B). The vast majority of up-regulated genes at the 3- and 4-day time points are involved with extracellular space and matrix roles (Fig. 10B). At 72 hr post bisection, hundreds of genes are up-regulated for biological processes, such as cell adhesion and lipid metabolism (Fig. 10B). Genes regulating small molecule and single organism metabolic processes on the other hand are down-regulated after 72 hr of regeneration, as well as numerous genes involved with oxidoreductase activity (Fig. 10B). Biological process genes aligned with aging, extracellular structure organization and matrix organization are down-regulated at the 96-hr time point (Fig. 10B). The cellular component categories of extracellular space and region part, as well as oxidoreductase activity in the molecular function category are also down-regulated at 96 hr post bisection (Fig. 10B).

Discussion

External Regeneration Morphology

Ptychoderid hemichordate regeneration is a remarkable process that results in external structures regenerating in an anterior to posterior manner patterned off the existing body axis. This is similar to juvenile worm development in *P. flava* and another ptychoderid hemichordate, *Balanoglossus simodensis*, when the proboscis forms first during metamorphosis (Miyamoto et al., 2010; Lin et al., 2016). The collar and trunk then differentiate and the trunk elongates. One difference between development and regeneration, however, is that gill slits start to regenerate before the collar has fully formed, unlike early development in direct developing hemichordates when gill slits form after the collar and trunk have delineated from one another (Kaul-Strehlow and Stach, 2013; Kaul-Strehlow et al., 2015).

Furthermore, during direct development, the neural tube also starts to invaginate from dorsal, collar ectoderm in the posterior region of the collar before the first gill slit formation (Kaul-Strehlow and Stach, 2013); however, we show in this study that the first gill slit regenerates at least 2 days before the neural tube begins to form in the indirect developing *P. flava*. Few studies directly compare development or regeneration of the neural tube and gill slits in ptychoderid worms, but two studies state that the collar develops or regenerates before the branchial region (Nielsen and Hay-Schmidt, 2007: Humphreys et al., 2010). This is not evidence that the neural tube specifically has developed at this point and future studies will need to confirm the timing of development of the neural tube compared with development of the branchial region in *P. flava*. These differences, however, do show a potential temporal plasticity during regeneration of anterior structures in *P. flava*.

During regeneration, cells proliferate and accumulate to form a blastema at the cut site, which then differentiate to replace

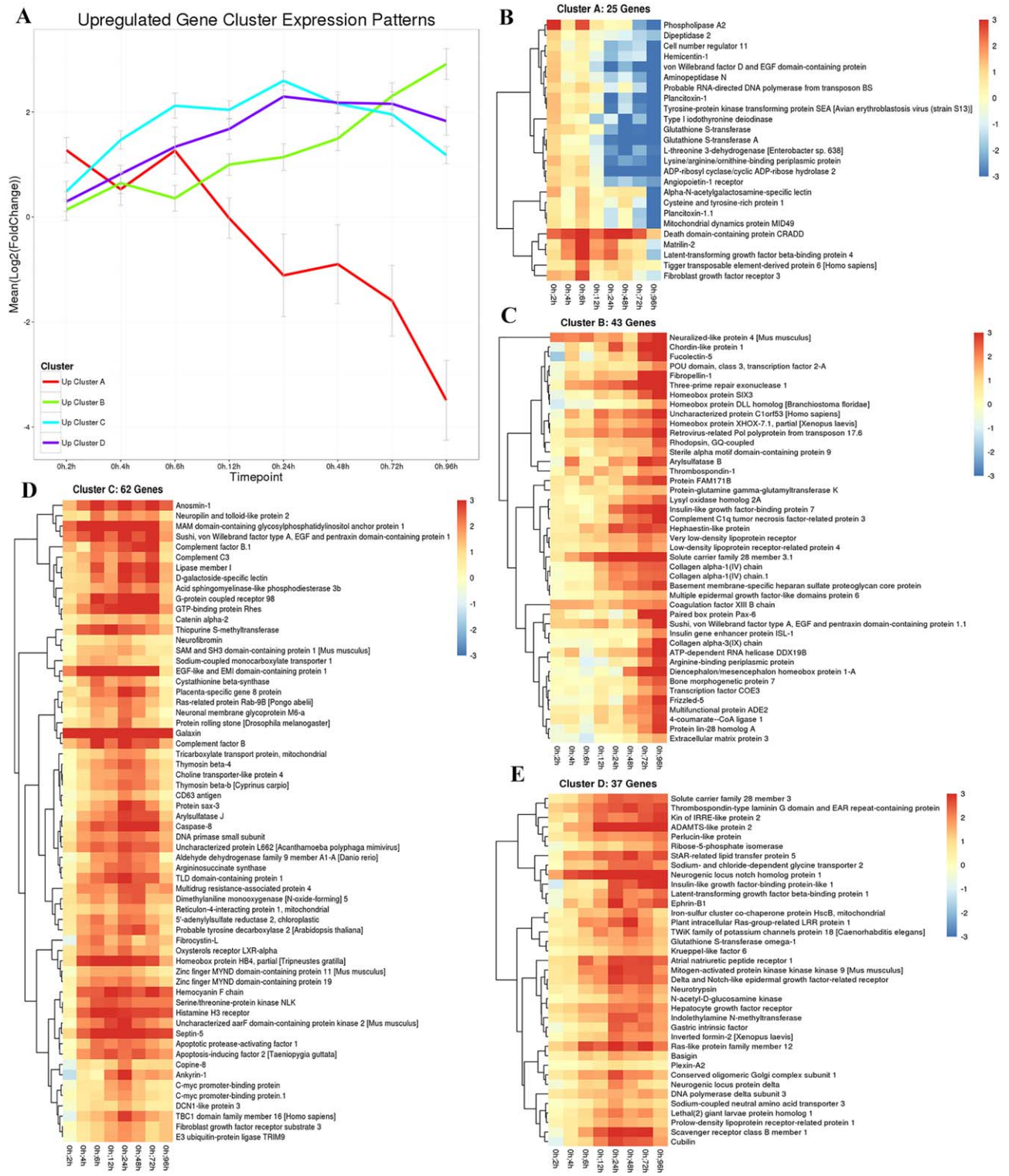

Fig. 5. Up-regulated gene cluster expression patterns in regenerating *Ptycodera flava*. **A:** The line graph shows all putative genes that are initially up-regulated and cluster together in their expression profiles along all time points sampled. Red, cluster A genes; green, cluster B genes; blue, cluster C genes; and purple, cluster D genes. The X-axis is time of regeneration and the Y-axis is the log2 fold change in gene expression compared with control animals. **B–E:** Heatmaps showing the individual genes identified in clusters A, B, C, D, respectively.

missing or damaged tissue. The question remains whether these proliferating cells are bona fide stem cells occupying an unknown niche that are recruited to the cut site or are these somatic cells that have undergone de-differentiation and returned to a progenitor cell state and then assigned new fates in the regenerating tissue? Numerous genes in *P. flava* are both up- and down-regulated beginning just 2 hr after the animal is bisected. Differential gene expression increases rapidly during the early time

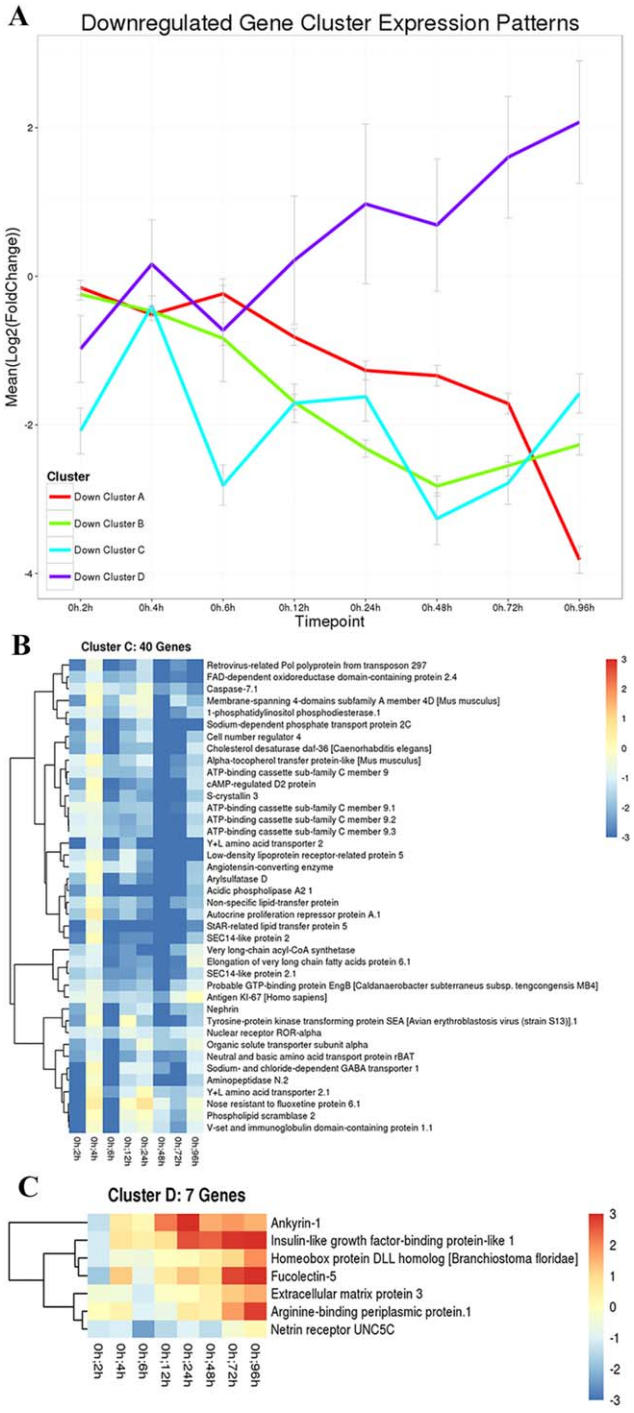

Fig. 6. Down-regulated gene cluster expression patterns in regenerating *Ptycodera flava*. **A:** The line graph shows all putative genes that are initially down-regulated and cluster together in their expression profiles along all time points sampled. Red, cluster A genes; green, cluster B genes; blue, cluster C genes; and purple, cluster D genes. The X-axis is time of regeneration and the Y-axis is the log2 fold change in gene expression compared with control animals. **B,C:** Heatmaps showing the individual genes in clusters C and D, respectively. Heatmaps and identities of genes in clusters A and B are included in Figures 7 and 8, respectively.

points sampled in this study resulting in wound healing and may drive regeneration through the recruitment of stem cells to the cut site forming the regeneration blastema within 3 to 4 days postamputation. Rychel and Swalla (2008) showed that proliferating cell nuclear antigen positive cells are found in scattered mesenchyme cells throughout the tissue near the cut site by day 2 of regeneration at 28°C in *P. flava*. There is some slight variation in wound healing and blastema growth times between the results reported by Rychel and Swalla (2008) and here, but the overall results are consistent. Our lab is currently working to determine the origin and molecular profile of these proliferating cells to verify whether these are stem cells or de-differentiated somatic cells. We are using stem cell markers in regenerating and nonregenerating animals to detect molecular signatures consistent with known stem cell lines.

Internal Regeneration Morphology

While epidermal tissue regenerates anterior to posterior, internal structures appear to regenerate based on need and function. The mouth, which is critical to feeding and thereby supports the high metabolic cost of regeneration, forms and opens after just 4 days. The worm does not burrow and ingest sand to deposit feed at this point; however, they are likely taking in organic nutrients suspended in the water column. Regenerating worms start to burrow in sand around 10 days postbisection. Blood vessels and mechanical support elements for vital organs and tissues also seem to be essential as these are among the first internal structures in the new tissue.

The stomochord in the posterior proboscis is vacuolated and acts as a hydrostatic skeleton, providing support for the heart-kidney complex (Miyamoto and Wada, 2013). Several studies have shown that, in both direct and indirect developing acorn worms, the stomochord is elaborated from endoderm during juvenile worm development (Kaul-Strehlow and Stach, 2013; Miyamoto and Wada, 2013; Satoh et al., 2014). At 3 days postbisection, we show what may be the presumptive stomochord regenerating from endoderm; however, the identity of this structure is not clear. At this stage, it is not positioned directly below the future heart/kidney complex in the proboscis as the stomochord should be, but rather it is more internal in the presumptive collar region. This structure could also be the hydropore, which is a rounded tube, but that is also not in the correct position, as the hydropore is in the dorsal proboscis/collar ectoderm region and expels circulating waste from the proboscis coelom to the environment (Röttinger and Martindale, 2011). It may be that the angle of the sections is not exactly sagittal, at which point internal structures may appear skewed. It may also be that regenerating structures look out of place during the early stages. Future studies will be needed using molecular markers to confirm the identity of this structure.

This study does clearly show, however, that the stomochord is elaborated from tissue at the ectoderm/endoderm boundary at 5 days postbisection. Tracing the anterior proboscis ectoderm to the anterior stomochord shows that ectoderm is definitely connected to this structure. Conversely, tracing the endodermal tissue to the posterior stomochord also shows that it is definitely connected to this tissue. So the question remains; at what point does endoderm become ectoderm? Our lab is using endodermal and ectodermal molecular markers to answer this provocative question and determine from what tissue type the stomochord regenerates.

The proboscis skeleton is cartilaginous and provides a rigid framework to protect the collar and overlying dorsal blood vessel and neural tube. The proboscis skeleton regenerates from

Fig. 7. Down-regulated gene cluster A expression patterns in regenerating *P. flava*. The heatmap shows the individual genes in cluster A of Figure 6 and their expression profile along all time points sampled compared with control animals.

endoderm, similar to early development (Luttrell et al., 2012; Miyamoto and Wada, 2013). A key difference is that the proboscis skeleton and dorsal vessel regenerate before neural tube regeneration. During normal development this process is reversed and the dorsal vessel and neural tube develop before the proboscis skeleton (Luttrell et al., 2012). Another major difference is the way the neural tube regenerates. During normal development, dorsal collar ectoderm invaginates, rolls up forming a hollow tube. During regeneration, the neural tube begins to form at day 13 as the collar ectoderm nears closure on the dorsal side. It is the closure of this ectoderm that actually forms the tube and not from invaginating ectoderm after the collar fully regenerates and closes.

This study shows that regeneration in *P. flava* does not strictly follow the developmental program and there are morphological steps that are regeneration specific. Furthermore, Arimoto and Tagawa (2015) showed that the *hedgehog* gene, which is highly conserved in the metazoans (Adamska et al., 2007) and involved

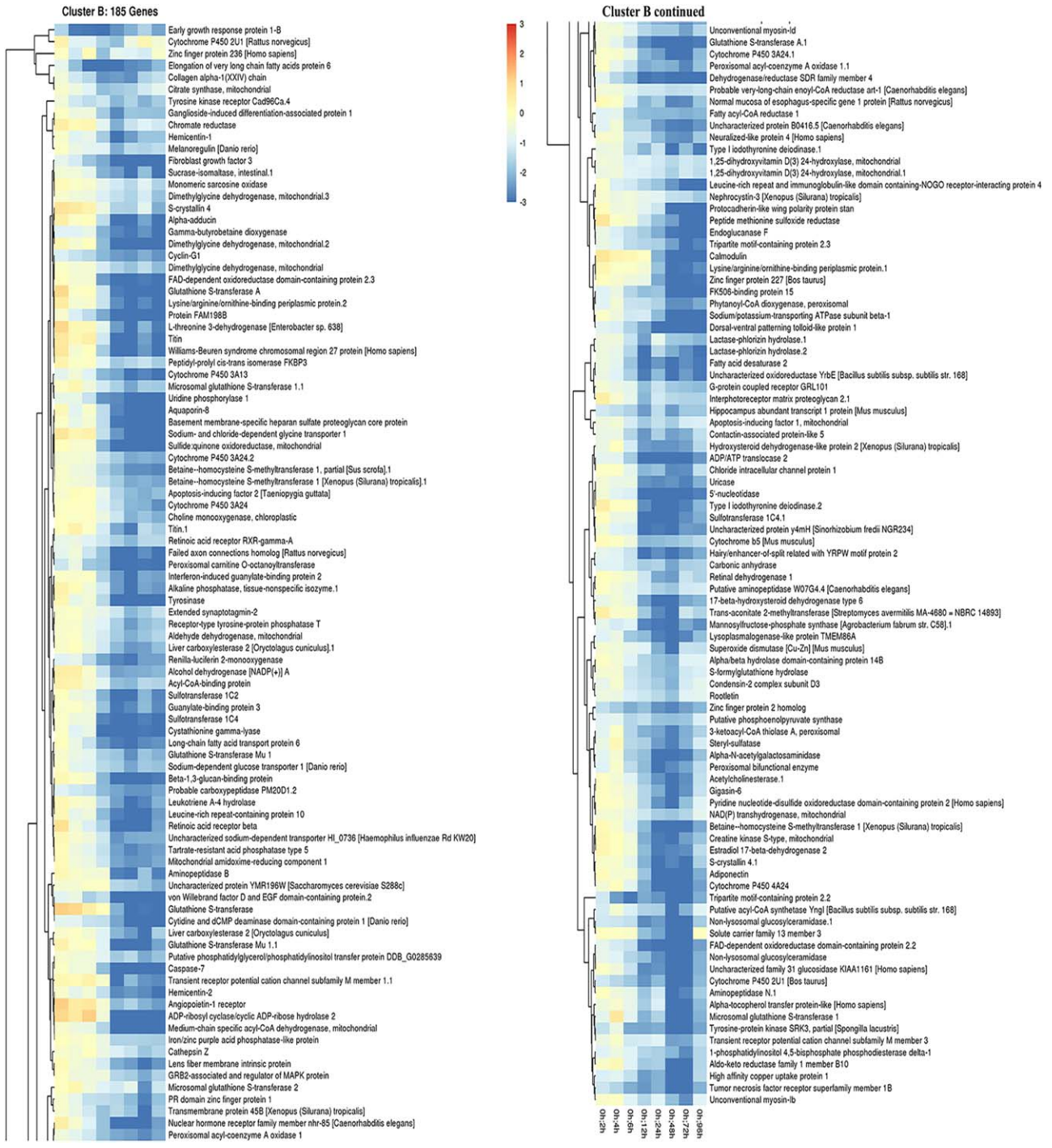

Fig. 8. Down-regulated gene cluster B expression patterns in regenerating *P. flava*. The heatmap shows the individual genes in cluster B of Figure 6 and their expression profile along all time points sampled compared with control animals.

with both morphogenesis and regeneration (Huangfu and Anderson, 2006; Rink et al., 2009), is expressed in both the pharyngeal endoderm and anterior tip of *P. flava* larvae, however, it is only expressed in the pharyngeal region during regeneration in *P. flava*. The regenerating proboscis tip does not express *hedgehog* and this evidence suggests there are different gene expression patterns that are regeneration specific in *P. flava* as well.

In the vertebrates, the notochord and dorsal vessel secrete signaling molecules to partially pattern the neural tube and peripheral nervous system, respectively. The notochord secretes sonic hedgehog, signaling the overlying ectoderm to become neural, invaginate and roll up forming the neural tube, while the dorsal blood vessel secretes bone morphogenetic protein molecules that signal neural crest cells to become peripheral neurons (Rickmann et al., 1985; Altaba et al., 1995; Briscoe et al., 1999; Schneider et al. 1999; Young et al., 2004). Hemichordates lack a notochord; therefore, the dorsal vessel may play a pivotal role in guiding CNS formation in the collar region during early

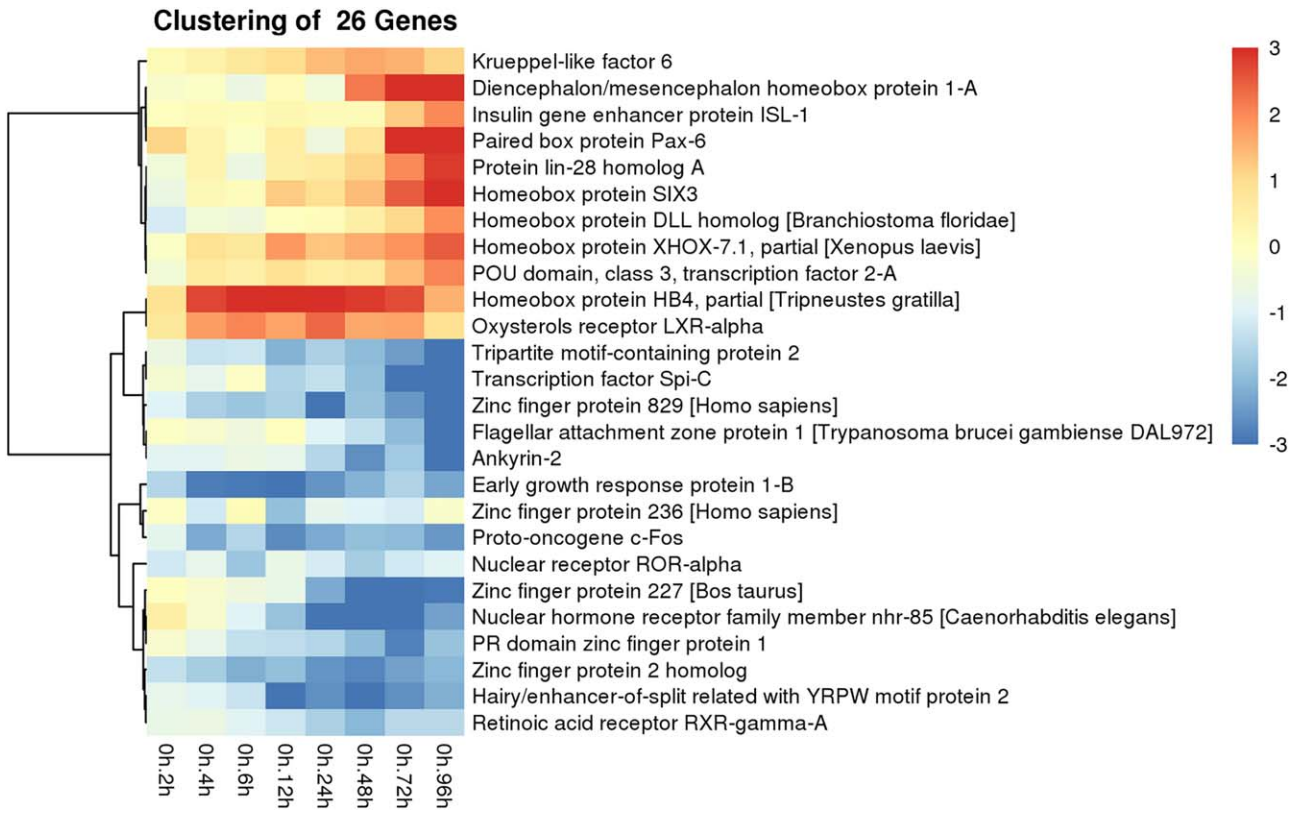

Fig. 9. Differential gene expression of putative transcription factors in regenerating *P. flava*. A heatmap showing the identity and expression profile of all transcription factors that were both up and down-regulated across all time points sampled compared with control animals.

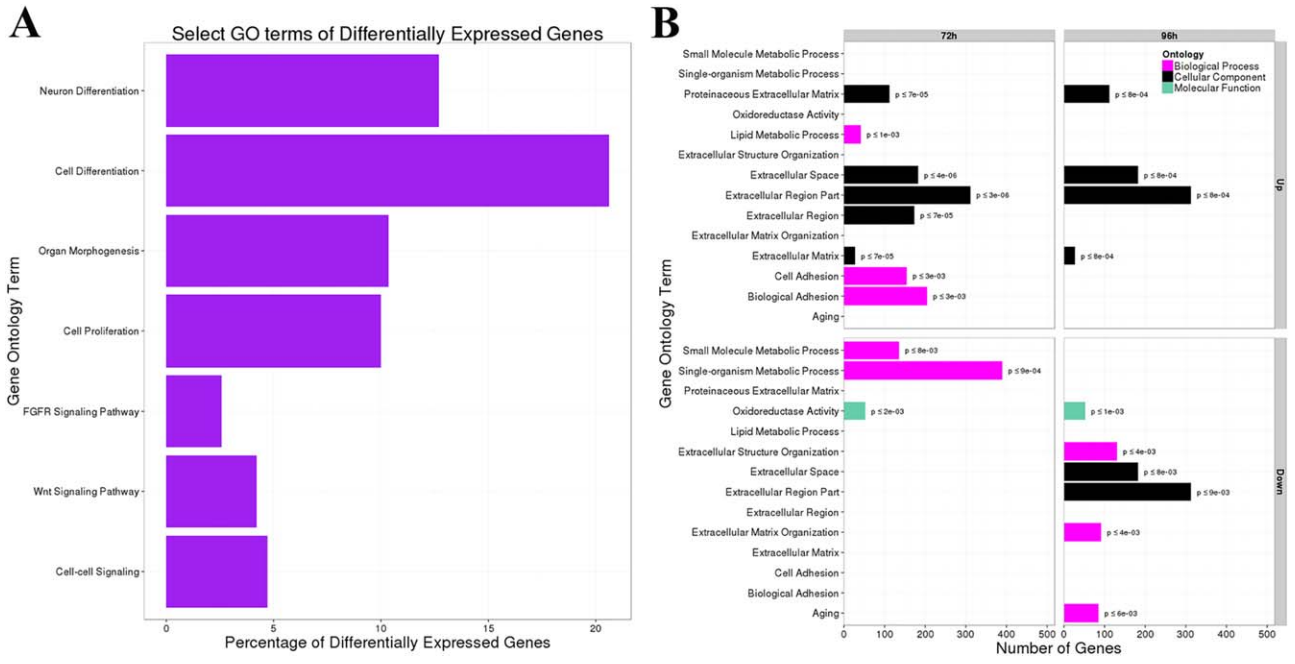

Fig. 10. Select GO terms of differentially expressed genes in regenerating *P. flava*. **A:** The X-axis is the percentage of genes that are differentially expressed in the biological processes on the Y-axis. **B:** The X-axis is the number of genes that were grouped into each gene ontology term on the Y-axis.

development. The dorsal vessel may still be directing this process during regeneration as this structure is formed and has regenerated into the proboscis by day 4. The tissue directly above the dorsal vessel in the collar region is thickened with a rich nerve net by 9 days postbisection and this tissue will become the ventral part of the neural tube. It is likely that signals directing a

neural tube fate are coming on early during collar regeneration, before the dorsal, collar ectoderm being present, and these signals may be emanating from the dorsal vessel.

Regeneration of the branchial region starts to occur before the collar closes dorsally and the neural tube forms. Between days 10 and 12, the first gill slit appears directly between the regenerating collar and the existing hepatic sacs. The regenerating branchial region in *P. flava* contains both pigmented and unpigmented cells. The anterior most branchial region closest to the collar is clear to white, while the posterior regenerating branchial region closest to the original cut site contains pigmented cells. Rychel and Swalla (2008) used a TUNEL (terminal deoxynucleotidyl transferase–mediated deoxyuridinetriphosphate nick end-labeling) assay to show numerous apoptotic cells in the endoderm of the hepatic sacs near the cut site 8 days after amputation. This suggests that, while the anterior most branchial tissue is likely elaborated from newly generated, unpigmented proliferating cells, the cells in the tissue closest to the cut site undergo apoptosis and the tissue is remodeled from the existing cells in the hepatic region. This hypothesis remains to be confirmed, but it will be exciting if internal structures regenerate using both stem cells and somatic cells in *P. flava* because it will provide a model to study two different modes of regenerating tissue in a stem deuterostome.

Expression of Putative Vertebrate Anterior Head Genes

Understanding the genetic and morphological basis of regeneration in hemichordates is vital to unlocking more extensive neural regeneration in humans. No vertebrate has been shown to be able to regenerate an anterior head or an entire CNS. Vertebrates that are capable of regenerating a small part of their CNS, like fish and amphibians (Slack et al., 2008; Sîrbulescu and Zupanc, 2010; Kroehne et al., 2011; Lau et al., 2013), possess numerous copies of single genes due to whole genome duplication events (Dehal and Boore, 2005; Hughes and Liberles, 2008). This genetic redundancy complicates functional studies of key genes controlling the regeneration process. Hemichordates not only lack whole genome duplications, but consistently regenerate their anterior head and complete CNS and, therefore, present a remarkable model system to study and uncover key genetic switches directing regeneration of anterior structures in the deuterostomes.

Several studies have detailed expression of genes involved with chordate brain and spinal cord development in the direct developing hemichordate, *Saccoglossus kowalevskii* (Lowe et al., 2003; Pani et al., 2012: Röttinger and Lowe, 2012). These orthologous genes show a similar spatial distribution of chordate patterning along the anterior–posterior body axis in *S. kowalevskii*. Numerous chordate forebrain genes are expressed in the developing hemichordate proboscis region while chordate midbrain genes are expressed in the hemichordate collar region and chordate hindbrain and spinal cord genes are expressed in the hemichordate trunk region (Lowe et al., 2003; Pani et al., 2012; Röttinger and Lowe, 2012). These overlapping similarities suggest that at least parts of the gene regulatory networks that pattern the chordate CNS were likely present in the common ancestor of the deuterostomes and the hemichordate proboscis and collar could be considered an early representation of the chordate head. No chordate has been shown to regenerate an anterior head or CNS after complete amputation and, therefore, hemichordates are vital to revealing gene networks regulating CNS regeneration in the deuterostomes.

We compared regeneration in *P. flava* and identified several putative orthologs of chordate CNS patterning genes that are up-regulated after 3 and 4 days of regeneration. The regeneration blastema has formed at these time points, and cells continue to proliferate to generate a rudimentary proboscis at 3 to 4 days postbisection of the animal. *Sine oculis homeobox 3 (six3)*, *distal-less (dll)*, *paired box homeobox 6 (pax6)*, and *frizzled-5* are all significantly up-regulated at the 96-hr time point, which is just as the proboscis begins to form. *Six3*, *Pax6*, and *dll* are transcription factors that are involved with patterning the chordate forebrain (Echevarria et al., 2003; Wilson and Houart, 2004; Paek et al., 2009). Frizzled-related Wnt antagonists have been shown to be necessary and sufficient to establish the telencephalon region of the chordate brain (Houart et al., 2002; Paek et al., 2009). Of the 26 putative transcription factors identified as being differentially expressed in this study, 7 of them are known to be involved in head and neural development and they are all significantly up-regulated 3 and 4 days into regeneration as the rudimentary proboscis is beginning to form. It is likely that other chordate head genes are up-regulated during anterior regeneration in *P. flava*, but they are possibly expressed at later time points as the proboscis continues to regenerate and the collar begins to form. Future studies will be aimed at identifying these transcripts and their expression domains.

Conclusions

We have shown that *Ptychodera flava* regeneration is not strictly a morphological recapitulation of development. There is extensive temporal plasticity during regeneration, as well as different modes of acquiring the same anterior structures. Putative orthologs of chordate head genes are also significantly up-regulated just before anterior proboscis regeneration. It will be interesting and informative to discover whether additional head genes are expressed as the proboscis and collar undergo regeneration and we will then use in situ hybridization to localize gene expression in regenerating tissues.

The origin of blastemal cells in *P. flava* still remains to be determined. Our lab is currently working to determine whether this animal uses genuine stem cells or dedifferentiated somatic cells to propagate missing tissue. In humans, when a cell differentiates into a particular cell type, the cell fate assignment normally cannot be reversed or transformed. If hemichordates are using dedifferentiated cells to elaborate new tissue, this may reveal cell signaling pathways necessary for the gain and loss of cell fates in the deuterostomes.

Experimental Procedures

Animal Collection and Management

Ptychodera flava were collected at Paiko Peninsula in Honolulu, Hawaii, in early November. During low tide, when the water level was approximately 3 feet deep, animals were removed from the coral beds by snorkeling. The light sand cover was fanned by hand to expose the underlying coral and hemichordates. Animals were collected into 50-ml tubes and carried back to the lab with the tubes immersed in a cooler with sea water.

Animals were bisected at the level of the anterior hepatic sacs and allowed to regenerate for various time points (Figs. 1 and 2). Regenerating worms were kept in running seawater tanks at Kewalo Marine Laboratory at 27°C during regeneration. Some worms were collected and shipped to the University of Washington in Seattle, Washington, and kept at 26°C while regenerating. Animals were immersed in a 1:1 solution of sea water and 7.5% $MgCl_2$ for 15 min to relax muscles and constrain movement and then observed with a Nikon 1000 dissecting microscope and photographed with a Cool Snap camera. Pictures were taken daily for 15 days and near daily thereafter until 55 days post bisection.

Histology

Regenerating animals were fixed in 4% paraformaldehyde in phosphate-buffered saline overnight at room temperature and stored at -20°C in 100% methanol. They were placed into 100% ethanol for, 20 min at room temperature and then moved to a 1:1 mixture of 100% ethanol and polyester wax (nine parts Poly (ethylene glycol) [400] distearate and one part 1-hexadecanol, (Polysciences, Warrington, PA) (Steedman, 1957; Norenburg and Barrett 1987) at 40°C for 1 hr. The animals were then moved to 100% polyester wax at 40°C for 1 hr and then embedded in fresh 100% polyester wax. Next, 7-μm sections were cut on a Spencer 829 microtome and mounted on gelatin subbed slides. Slides were deparaffinized, and processed through Milligan's trichrome staining, a histological stain that differentiates muscle cells, nuclei, and cartilage (Fig. 3; Presnell and Schreibman, 1997). Slides were rinsed in 95% ethanol and treated for 5 min with potassium dichromate HCl mordant and then rinsed in distilled water. Slides were then stained for 5 min in acid fuchsin (Sigma, St. Louis, MO) and rinsed again in distilled water. Slides were then stained 5 min in phosphomolybdic acid (Sigma) followed by 5 min in Orange G (Sigma) and then rinsed in distilled water. Finally, slides were treated for 2 min in 1% glacial acetic acid and stained 5 min with Fast Green FCF (Sigma) and then treated again for 3 min with 1% glacial acetic acid. Slides were dehydrated with ethanol and mounted with Permount (Fisher Scientific, Pittsburgh, PA). Sections were photographed using a Nikon Eclipse E600 microscope mounted with a Cool Snap camera.

RNA Isolation and cDNA Preparation

Following bisection, animals were allowed to regenerate for either 2 hr, 4 hr, 6 hr, 12 hr, 24 hr, 48 hr, 72 hr, or 96 hr. Between 50 and 100 mg of tissue were removed with a sterile, feather surgical blade from the cut site of the posterior segment in four regenerating animals at each time point (Fig. 1A–C). Four healthy, intact animals were bisected and total RNA was isolated from the cut site of the posterior half to serve as reference controls. RNA was isolated from the tissue using either a Promega SV Total RNA Isolation System, catalog number Z3100, or a USB PrepEase RNA Spin Kit, part number 78766 1 KT. RNA was analyzed on a NanoDrop ND-1000 spectrophotometer for nucleic acid concentration and purity and then stored at -80°C until cDNA was synthesized using the SuperScript® III First-Strand Synthesis System for RT-PCR by Invitrogen.

cDNA Library Preparation and Sequencing

mRNAseq libraries for sequencing were generated from 1 to 1.5 μg of high quality total RNA, as assessed using the Agilent 2100 Bioanalyzer. RNA was purified using poly-T oligo-attached magnetic beads. Libraries were made according to the manufacturer's directions for the TruSeq RNA Sample Prep Kit v2 (Illumina, RS-122-2101). Resulting short fragment libraries were checked for quality and quantity using the Bioanalyzer. Equal molar libraries were pooled, requantified and sequenced as 100 bp paired read on the Illumina HiSeq, 2000 instrument using HiSeq Control Software 1.5.15. Following sequencing, Illumina Primary Analysis version RTA 1.13.48 and Secondary Analysis version CASAVA-1.8.2 were run to demultiplex reads for all libraries and generate FASTQ files.

Transcriptome Assembly and Annotation

To create a reference for expression analysis, paired end sequence files from all *P. flava* experimental time points were pooled (605,821,125 pairs totaling 122,164,225,000 bp) and assembled using Trinity, version r2013-02-25, (Grabherr et al., 2011), with default parameters. We vector clipped and contaminate filtered the resulting assembly with SeqClean, version, 2011-02-22, (SeqClean, 2011). The resulting transcriptome reference contained 527,715 sequences, with an average length of 1,022, and N50 of 1,961, 208,773 of these sequences contain an ORF of at least 60 amino acids. All sequences were used for expression analysis with sequences from the same Trinity "component," roughly equal to a gene, treated as a single gene.

To maximize the utility of this transcriptome assembly, sequences were annotated with the best BLASTx (Camacho et al., 2008) hit to Swissprot (UniProt, 2015) and NCBI's NR database, using an e-value cutoff of 0.001. We also identified PFAM (Finn et al., 2014) domains present in *P. flava* transcripts using hmmscan, version 3.1b1, from the HMMER package (Eddy, 2011) with an e-value cutoff of 0.01. In addition, we annotated these transcripts with tmhmm, version 2.0c, (Krogh et al., 2001) signalP version 4.1 (Petersen et al., 2011), and ncoils (Lupas et al., 1991). We identified putative transcription factors based on PFAM domain hits using a list from transcriptionfactor.org. For transcripts with multiple isoforms, annotations were collapsed to the gene level as determined by Trinity.

Differential Expression Analysis

To identify differentially expressed genes, single end reads from each time point were aligned to the transcriptome using Bowtie2 (Langmead and Salzberg, 2012) with default parameters. Alignments were quantified using Samtools (Li et al., 2009). Isoform counts were summed to generate a "per gene" count. Differential expression analysis and normalization was performed using the R package DESeq2 (Love et al., 2014). All time points were contrasted with the zero hour (0 hr) time point. Data used for the gene expression analysis have been deposited in the Gene Expression Omnibus (GEO) under accession number GSE70295.

Hierarchical Clustering and Heatmaps

To select genes of interest for clustering, differentially expressed genes ($P < 1e\text{-}5$), having an expression level log2 fold change greater than one or less than negative one, for one or more time

points, and having a hit to the Swissprot protein database were identified. These genes were hierarchically clustered on the distances of the Pearson correlation of the log2 fold change, using the complete linkage method to find similar clusters (Figs. 5 and 6, 7, 8). Significantly differentially expressed genes ($P < 1e\text{-}5$) that had transcription factor domains were clustered on the distances of the Pearson correlation of the log2 fold change, using Ward's minimum variance method to find similar clusters (Fig. 9). All heatmaps were created using the R package pheatmap (Kolde, 2013).

Gene Ontology Analysis

Gene Ontology (GO) (Gene Ontology, 2015) terms were assigned to each *P. flava* gene based upon homologous PFAM domains and significant Swissprot hits. These terms were used to impute functional categories of differentially expressed genes and calculate categorical enrichment. The GO slim terms used were from the generic GO slim terms list available at the Gene Ontology Web site. GO term enrichment was performed using the R package topGO (Alexa and Rahnenfuhrer, 2010). To examine higher-level GO terms, significantly enriched ($P < 0.01$) GO terms were mapped to select higher-level GO terms using GO.db. These select GO terms were then mapped to the significantly differentially expressed genes ($P < 1e\text{-}5$) (Fig. 10).

Acknowledgments

We thank Dr. Michael Hadfield for allowing us to use his seawater tanks, microscopes, and lab space at Kewalo Marine Laboratory. We also thank the Seeley family for their encouragement and their generous donation from the Seeley Fund for Ocean Research on Tetiaroa. This work was also funded in part by NIH to Dr. Alejandro Sánchez Alvarado. Dr. Alejandro Sánchez Alvarado is a Howard Hughes Medical Institute and Stowers Institute for Medical Research Investigator. This material is based upon work supported by the National Science Foundation Graduate Research Fellowship Program to Shawn Luttrell. Additionally, this material is also based in part upon work supported by the National Science Foundation. Any opinions, findings, and conclusions or recommendations expressed in this material are those of the author(s) and do not necessarily reflect the views of the National Science Foundation. Shawn Luttrell is a Ph.D. candidate in the Swalla Lab at the University of Washington and collected all animals and performed all regeneration experiments, RNA isolation, sectioning and histology, constructed the figures, and wrote the manuscript, including the figure legends. Dr. Billie J. Swalla is a Principal Investigator and oversaw all aspects of animal collection and disposition, regeneration experiments, histology, and manuscript preparation and editing. Dr. Alejandro Sánchez Alvarado is a Principal Investigator at the Stowers Institute for Medical Research in Kansas City, Missouri, and oversaw all aspects of the sequencing, assembly, and annotation of the transcriptome. Eric Ross is a Bioinformatics Specialist in the Sánchez Lab who, along with Kirsten Gotting, a Bioinformaticist also in the Sánchez Lab assembled and analyzed the transcriptome data. They also wrote the methods for the transcriptome sequencing, assembly and annotation and generated the heatmaps, transcriptome line graphs, and gene ontology graphs. All authors were involved in the writing of this manuscript and page proofs. S.M.L. was funded by the DGE, A.S.A. was funded by the NIH and HHMI, B.J.S was funded by the DBI, and B.J.S. and S.M.L. were funded by the Seeley Fund for Ocean Research on Tetiaroa

References

Adamska M, Matus DQ, Adamski M, Green K, Rokhsar DS, Martindale MQ, Degnan BM. 2007. The evolutionary origin of hedgehog proteins. Curr Biol 17:R836–R837.

Alexa A, Rahnenfuhrer J. 2010. topGO: topGO: enrichment analysis for gene ontology. R package version 2.20.0.

Altaba A, Jessel TM, Roelink H. 1995. Restrictions to floor plate induction by hedgehog and winged-helix genes in the neural tube of frog embryos. Mol Cell Neurosci 6:106–121.

Arimoto A, Tagawa K. 2015. Hedgehog expression during development and regeneration in the hemichordate, Ptychodera flava. Zoolog Sci 32:33–37.

Balser EJ, Ruppert EE. 1990. Structure, ultrastructure, and function of the preoral heart-kidney in Saccoglossus kowalevskii (Hemichordata, Enteropneusta) including new data on the stomochord. Acta Zool 71:235–249.

Bely AE, Nyberg KG. 2010. Evolution of animal regeneration: re-emergence of a field. Trends Ecol Evol 25:161–170.

Benito J, Pardos F. 1997. Hemichordata. In: F Harrison F, Ruppert E, editors. Microscopic anatomy of invertebrates, Vol. 15, New York: Wiley-Liss. p 15–101.

Bosch TCG. 2007. Why Polyps regenerate and we don't: towards a cellular and molecular framework for Hydra regeneration. Dev Biol 303:421–433.

Briscoe J, Sussel L, Serup P, Hartigan-O'Connor D, Jessell TM, Rubenstein JL, Ericson J. 1999. Homeobox gene Nkx2.2 and specification of neuronal identity by graded Sonic hedgehog signaling. Nature 398:622–627.

Brown FD, Keeling EL, Le AD, Swalla BJ. 2009. Whole body regeneration in a colonial ascidian, Botrylloides violaceus. J Exp Zool B Mol Dev Evol 312B:885–900.

Brown FD, Prendergast A, Swalla BJ. 2008. Man is but a worm: chordate origins. Genesis 46:605–613.

Brown RC, Lockwood AH, Sonawane BR. 2005. Neurodegenerative diseases: an overview of environmental risk factors. Environ Health Perspect 113:1250–1256.

Candia Carnevali MD, Thorndyke MC, Matranga V. 2009. Regenerating in echinoderms: a promise to understand stem cells potential. In: Rinkevich B, Matranga V, editors. Stem cells in marine organisms. New York: Springer. p 165–186.

Camacho C, Coulouris G, Avagyan V, Ma N, Papadopoulos J, Bealer K, Madden TL. 2008. BLAST+: architecture and applications. BMC Bioinformatics 10:421.

Dahlberg C, Auger H, Dupont S, Sasakura Y, Thorndyke M, Joly J-S. 2009. Refining the Ciona intstinalis model of central nervous system regeneration. PLoS One 4:e4458. doi:10.1371/journal.pone.0004458.

Dawydoff C. 1902. Utber die Regeneration der Eichel bei den Enteropneusten. Zool Anz 25:551–556.

Dehal P, Boore J. 2005. Two rounds of whole genome duplication in the ancestral vertebrate. Plos Biol 3:1700–1708.

Dubuc TQ, Traylor-Knowles N, Martindale MQ. 2014. Initiating a regenerative response, cellular and molecular features of wound healing in the cnidarian Nematostella vectensis. BMC Biol 12:24.

Echevarria D, Vieira C, Gimeno L, Martinez S. 2003. Neuroepithelial secondary organizers and cell fate specification in the developing brain. Brain Res Brain Res Rev 43:179–191.

Eddy SR. 2011. Accelerated profile HMM searches. PLoS Comp Biol 7:e1002195.

Eschscholtz F. 1825. Bericht über die zoologische Ausbeute während der Reise von Kronstadt bis St. Peter und Paul. Isis 733–747. Available at: http://www.biodiversitylibrary.org/item/87983#page/403/mode/1up

Finn RD, Bateman A, Clements J, Coggill P, Eberhardt RY, Eddy SR, Heger A, Hetherington K, Holm L, Mistry J, Sonnhammer ELL, Tate J, Punta M. 2014. Pfam: the protein families database. Nucleic Acids Res 42:D222–D230.

Gene Ontology C. 2015. Gene Ontology Consortium: going forward. Nucleic Acids Res 43:D1049–D1056.

Giangrande A, Licciano M. 2014. Regeneration and clonality in Metazoa. The price to pay for evolving complexity. Invertebr Reprod Dev 58:1–8.
Grabherr MG, Haas BJ, Yassour M, Levin JZ, Thompson DA, Amit I, Adiconis X, Fan L, Raychowdhury R, Zeng Q, Chen Z, Mauceli E, Hacohen N, Gnirke A, Rhind N, di Palma F, Birren BW, Nusbaum C, Lindblad-Toh K, Friedman N, Regev A. 2011. Full-length transcriptome assembly from RNA-seq data without a reference genome. Nat Biotechnol 29:644–652.
Hadfield MG. 1978. Growth and metamorphosis of planktonic larvae of Ptychodera flava (Hemichordata: Enteropneusta). In: Chia FS, Rice ME, editors. Settlement and metamorphosis of marine invertebrate larvae. New York: Elsevier. p 247–254.
Holland L, Carvalho J, Escriva H, Laudet V, Schubert M, Shimeld SM, Yu J. 2013. Evolution of bilaterian central nervous systems: a single origin? Evodevo 4:27.
Houart C, Caneparo L, Heisenberg C, Barth K, Take-Uchi M, Wilson SW. 2002. Establishment of the telencephalon during gastrulation by local antagonism of Wnt signaling. Neuron 35: 255–265.
Huangfu D, Anderson KV. 2006. Signaling from Smo to Ci/Gli: conservation and divergence of Hedgehog pathways from Drosophila to vertebrates. Development 133:3–14.
Hughes T, Liberles D. 2008. Whole-genome duplications in the ancestral vertebrate are detectable in the distribution of gene family sizes of tetrapod species. J Mol Evol 67:343–357.
Humphreys T, Sasaki A, Uenishi G, Taparra K, Arimoto A, Tagawa K. 2010. Regeneration in the hemichordate Ptychodera flava. Zoolog Sci 27:91–95.
Kaul S, Stach T. 2010. Ontogeny of the collar cord: neurulation in the hemichordate Saccoglossus kowalevskii. J Morphol 271: 1240–1259.
Kaul-Strehlow S, Stach T. 2013. A detailed description of the development of the hemichordate Saccoglossus kowalevskii using SEM, TEM, histology and 3D-reconstructions. Front Zool 10:53.
Kaul-Strehlow S, Urata M, Minokawa T, Stach T, Wanninger A. 2015. Neurogenesis in directly and indirectly developing enteropneusts: of nets and cords. Org Divers Evol 15:405–422.
Kolde R. 2013. pheatmap: pretty heatmaps. R package version 0.7.7. Available at: http://CRAN.R-project.org/package=pheatmap.
Krogh A, Larsson B, von Heijne G, Sonnhammer ELL. 2001. Predicting transmembrane protein topology with a hidden Markov model: application to complete genomes. J Mol Biol 305:567–580.
Kroehne V, Freudenreich D, Hans S, Kaslin J, Brand M. 2011. Regeneration of the adult zebrafish brain from neurogenic radial glia-type progenitors. Development 138:4831–4841.
Langmead B, Salzberg S. 2012. Fast gapped-read alignment with Bowtie 2. Nat Methods 9:357–359.
Lau BYB, Fogerson SM, Walsh RB, Morgan JR. 2013. Cyclic AMP promotes axon regeneration, lesion repair and neuronal survival in lampreys after spinal cord injury. Exp Neurol 250:31–42.
Li H, Handsaker B, Wysoker A, Fennell T, Ruan J, Homer N, Marth G, Abecasis G, Durbin R, 1000 Genome Project Data Processing Subgroup. 2009. The Sequence alignment/map (SAM) format and SAMtools. Bioinformatics 25:2078–2079.
Lin CY, Tung CH, Yu JK, Su YH. 2016. Reproductive periodicity, spawning induction, and larval metamorphosis of the hemichordate acorn worm Ptychodera flava. J Exp Zool B Mol Dev Evol 326:47–60.
Love MI, Huber W, Anders S. 2014. Moderated estimation of fold change and dispersion for RNA-seq data with DESeq2. Genome Biol 15:550.
Lowe CJ, Wu M, Salic A, Evans L, Lander E, Stange-Thomann N, Gruber CE, Gerhart J, Kirschner M. 2003. Anteroposterior patterning in hemichordates and the origins of the chordate nervous system. Cell 113:853–865.
Lupas A, Van Dyke M, Stock J. 1991. Predicting coiled coils from protein sequences. Science 252:1162–1164.
Luttrell S, Konikoff C, Byrne A, Bengtsson B, Swalla B. 2012. Ptychoderid hemichordate neurulation without a notochord. Integr Comp Biol 52:829–834.
Luttrell SM, Swalla BJ. 2014. Genomic and evolutionary insights into chordate origins. In: Moody S, editor. Principles of developmental genetics, 2nd ed. San Diego: Elsevier. p 116–126.
Mahabaleshwarkar R, Khanna R. 2014. National hospitalization burden associated with spinal cord injuries in the United States. Spinal Cord 52:139–144.
Miyamoto N, Saito Y. 2010. Morphological characterization of the asexual reproduction in the acorn worm Balanoglossus simodensis. Dev Growth Differ 52:615–627.
Miyamoto N, Nakajima Y, Wada H, Saito Y. 2010. Development of the nervous system in the acorn worm Balanoglossus simodensis: insights into nervous system evolution. Evol Dev 12:416–424.
Miyamoto N, Wada H. 2013. Hemichordate neurulation and the origin of the neural tube. Nat Commun 4:1–8.
Morgan T. 1894. The development of Balanoglossus. J Morphol 9: 1–86.
Moroz LL, Kocot KM, Citarella MR, Dosung S, Norekian TP, Povolotskaya IS, Grigorenko AP, Dailey C, Berezikov E, Buckley KM, Ptitsyn A, Reshetov D, Mukherjee K, Moroz TP, Bobkova Y, Yu F, Kapitonov VV, Jurka J, Bobkov YV, Swore JJ, Girardo DO, Fodor A, Gusev F, Sanford R, Bruders R, Kittler E, Mills CE, Rast JP, Derelle R, Solovyev VV, Kondrashov FA, Swalla BJ, Sweedler JV, Rogaev EI, Halanych KM, Kohn AB. 2014. The ctenophore genome and the evolutionary origins of neural systems. Nature 510:109–114.
Nielsen C, Hay-Schmidt A. 2007. Development of the Enteropneust Ptychodera flava: ciliary bands and nervous system. J Morphol 268:551–570.
Nishikawa T. 1977. Preliminary report on the biology of the enteropneust, Ptychodera flava Eschscholtz, in the vicinity of Kushimoto, Japan. Publ Seto Marine Biol Lab 23:393–419.
Norenburg JL, Barrett JM. 1987. Steedman's polyester wax embedment and deembedment for combined light and scanning electron microscopy. J Electron Microsc Tech 6:35–41.
Paek H, Gutin G, Hebert JM. 2009. FGF signaling is strictly required to maintain early telencephalic precursor cell survival. Development 136:2457–2465.
Pani AM, Mullarkey EE, Aronowicz J, Assimacopoulos S, Grove EA, Lowe CJ. 2012. Ancient deuterostome origins of vertebrate brain signaling centers. Nature 483:289–294.
Petersen TN, Brunak S, von Heijne G, Nielsen H. 2011. SignalP 4.0: discriminating signal peptides from transmembrane regions. Nat Methods 8:785–786.
Presnell JK, Schreibman MP. 1997. Humason's animal tissue techniques. Baltimore: Johns Hopkins University Press. 572 p.
Rando TA, Wyss-Coray T. 2014. Stem cells as vehicles for youthful regeneration of aged tissues. J Gerontol A Biol Sci Med Sci 69: S39–S42.
Rao K. 1954. The early development of an Enteropneusta Ptychodera flava Eschsholtz. J Zool Soc India 6:145–152.
Rickmann M, Fawcett J, Keynes R. 1985. The migration of neural crest cells and the growth of motor axons through the rostral half of the chick somite. J Embryol Exp Morphol 90:437–55.
Rink JC, Gurley KA, Elliott SA, Alvarado AS. 2009. Planarian Hh signaling regulates regeneration polarity and links Hh pathway evolution to cilia. Science 326:1406–1410.
Röttinger E, Lowe CJ. 2012. Evolutionary crossroads in developmental biology: hemichordates. Development 139:2463–2475.
Röttinger E, Martindale MQ. 2011. Ventralization of an indirect developing hemichordate by $NiCl_2$ suggests a conserved mechanism of dorso-ventral (D/V) patterning in Ambulacraria (hemichordates and echinoderms). Dev Biol 354:173–190.
Ryan JF, Pang K, Schnitzler CE, Nguyen AD, Moreland RT, Simmons DK, Koch BJ, Francis WR, Havlak P, Smith SA, Putnam NH, Haddock SH, Dunn CW, Wolfsberg TG, Mullikin JC, Martindale MQ, Baxevanis AD. 2013. The genome of the ctenophore Mnemiopsis leidyi and its implications for cell type evolution. Science 342:1242592.
Rychel AL, Swalla BJ. 2008. Anterior regeneration in the hemichordate Ptychodera flava. Dev Dyn 237:3222–3232.
Sánchez Alvarado A. 2000. Regeneration in the metazoans: why does it happen? Bioessays 22:578–590.

Satoh N, Tagawa K, Lowe CJ, Yu JK, Kawashima T, Takahashi H, Ogasawara M, Kirschner M, Hisata K, Su YH, Gerhart J. 2014. On a possible evolutionary link of the stomochord of hemichordates to pharyngeal organs of chordates. Genesis 52:925–934.
Schneider C, Wicht H, Enderich J, Wegner M, Rohrer H. 1999. Bone morphogenetic proteins are required in vivo for the generation of sympathetic neurons. Neuron 24:861–70.
SeqClean. 2011. Available at: http://sourceforge.net/projects/seqclean/.
Chen SH, Li KL, Lu IH, Wang YB, Tung CH, Ting HC, Lin CY, Lin CY, Su YH, Yu JK. 2014. Sequencing and analysis of the transcriptomes of the acorn worm Ptychodera flava, an indirect developing hemichordate. Mar Genomics 15:35–43.
Simakov O, Kawashima T, Marlétaz F, Jenkins J, Koyanagi R, Mitros T, Hisata K, Bredeson J, Shoguchi E, Gyoja F, Yue JX, Chen YC, Freeman RM Jr, Sasaki A, Hikosaka-Katayama T, Sato A, Fujie M, Baughman KW, Levine J, Gonzalez P, Cameron C, Fritzenwanker JH, Pani AM, Goto H, Kanda M, Arakaki N, Yamasaki S, Qu J, Cree A, Ding Y, Dinh HH, Dugan S, Holder M, Jhangiani SN, Kovar CL, Lee SL, Lewis LR, Morton D, Nazareth LV, Okwuonu G, Santibanez J, Chen R, Richards S, Muzny DM, Gillis A, Peshkin L, Wu M, Humphreys T, Su YH, Putnam NH, Schmutz J, Fujiyama A, Yu JK, Tagawa K, Worley KC, Gibbs RA, Kirschner MW, Lowe CJ, Satoh N, Rokhsar DS, Gerhart J. 2015. Hemichordate genomes and deuterostome origins. Nature 527: 459–465.
Sîrbulescu R, Zupanc G. 2010. Spinal cord repair in regeneration-competent vertebrates: adult teleost fish as a model system. Brain Res Rev 67:73–93.
Slack JMW, Lin G, Chen Y. 2008. The Xenopus tadpole: a new model for regeneration research. Cell Mol Life Sci 65:54–63.
Sly BJ, Hazel JC, Popodi EM, Raff RA. 2002. Patterns of gene expression in the developing adult sea urchin central nervous system reveal multiple domains and deep-seated neural pentamery. Evol Dev 4:189–204.
Somorjai IML, Somorjai RL, Garcia-Fernandez J, Escriva H. 2012. Vertebrate-like regeneration in the invertebrate chordate amphioxus. Proc Natl Acad Sci U S A 109:517–522.
Steedman HF. 1957. Polyester wax: a new ribboning embedding medium for histology. Nature 179:1345.
Tagawa K, Arimito A, Sasaki A, Izumi M, Fujita S, Humphreys T, Fujiyama A, Kagoshima H, Shin-I T, Kohara Y, Satoh N, Kawashima T. 2014. A cDNA resource for gene expression studies of a hemichordate, Ptychodera flava. Zoolog Sci 31:414–420.
UniProt C. 2015. UniProt: a hub for protein information. Nucleic Acids Res 43:D204–D212.
Willey A. 1899. Enteropneusta from the South Pacific, with notes on the West Indian Species. In: Willey A, editor. Zoological results, Part 3. Cambridge.
Wilson SW, Houart C. 2004. Early steps in the development of the forebrain. Dev Cell 6:167–181.
Young HM, Anderson RB, Anderson CR. 2004. Guidance cues involved in the development of the peripheral autonomic nervous system. Auton Neurosci 112:1–14.
Ziegler-Graham K, MacKenzie EJ, Ephraim PL, Travison TG, Brookmeyer R. 2008. Estimating the Prevalence of Limb Loss in the United States: 2005 to 2050. Arch Phys Med Rehabil 89: 422–429.